Optics Communications 392 (2017) 171–174

Contents lists available at ScienceDirect

Optics Communications

journal homepage: www.elsevier.com/locate/optcom

Measuring the branching ratios from the $y^8P_{9/2}$ state to metastable states in europium

Yuki Miyazawa, Ryotaro Inoue, Keiji Nishida, Toshiyuki Hosoya, Mikio Kozuma*

Department of Physics, Tokyo Institute of Technology, 2-12-1 O-Okayama, Meguro-ku, Tokyo 152-8550, Japan

ARTICLE INFO

MSC:
70-05

Keywords:
Europium
Laser cooling
Branching ratio
Dipolar gas

ABSTRACT

We measure the branching ratios from the $y^8P_{9/2}$ excited state to six metastable states of europium through fluorescence spectroscopy of an atomic beam. The sum of the six branching ratios is estimated to be $1.05(2) \times 10^{-3}$. This research provides us with insightful information to determine the feasibility of using the $a^8S_{7/2} - y^8P_{9/2}$ transition in order to implement the Zeeman slowing for europium atoms in the ground state. Based on this result, we also propose a scheme for Zeeman slowing and magneto-optical trapping, using a specific metastable state which has a cyclic transition.

1. Introduction

Ultracold atoms with a large magnetic dipole moment μ are useful to study a new class of strongly correlated physics relying on magnetic dipole-dipole interaction (MDDI). Many exciting phenomena based on the long-range and anisotropic nature of the interaction have been studied and pave the way for recent investigations such as supersolid [1,2], quantum magnetism [3–5], and spontaneous spin textures [6–8]. So far, strongly dipolar atomic species of chromium (Cr, $\mu = 6$ Bohr magneton, μ_B), dysprosium (Dy, $\mu = 10\,\mu_B$), and erbium (Er, $\mu = 7\,\mu_B$) have been brought to quantum degeneracy [9–11]. Rich dipolar phenomena have been observed and studied with these systems, such as the d-wave collapse of the dipolar Bose-Einstein condensate [12], the deformation of the Fermi surface [13], and the droplets stabilized by quantum fluctuations [14–17]. These experiments are performed under DC magnetic field for fixing spin direction, whereas fascinating phenomena can also be expected under ultra-low magnetic field. The MDDI couples spins and orbital angular momenta, which are believed to produce rich ground-state phases including spin textures and vortices [6–8,18].

Europium (Eu), which has not been laser-cooled yet, is a good candidate for investigating such ground-state phases. It has large dipole moment ($7\,\mu_B$) and two stable bosonic isotopes, ^{151}Eu (natural abundance: 48%) and ^{153}Eu (52%), where both the isotopes have the same nuclear spins $I = 5/2$. Europium also has zero-electronic-orbital ground state in contrast to the other dipolar lanthanides, whose large electronic orbital provides a strong anisotropy and the resultant rich scattering behavior [19]. As with the case of conventional ultracold alkaline atoms, a scattering length of Eu is expected to be well-controlled by using magnetic-field induced Feshbach resonance [20]. In addition, the s-wave scattering length can in principle be controlled by using the microwave-induced Feshbach resonance [21,22] even under zero magnetic field. Note that the bosonic isotopes of Cr, Dy, and Er do not have hyperfine structures in their ground states. Holmium (Ho), which has recently been laser-cooled [23], is one of the good candidates since it has large dipole moment ($9\,\mu_B$) and a stable bosonic isotope (^{165}Ho) with non-zero nuclear spin. However, there is a concern about the inelastic loss due to hyperfine exchanging collision [24] in the investigation of the ground-state phases using ultracold Ho atoms, since its hyperfine state with maximum magnetic moment does not correspond to the lowest energy one in contrast to the case of Eu.

Magneto-optical trapping (MOT) is the first building block to bring the Eu atoms into quantum degeneracy. A hot effusive oven is one of the most promising sources providing enough atomic flux, since Eu has almost zero vapor pressure at room temperature [25]. The hot atomic beam should be decelerated by the Zeeman slowing technique using a cyclic transition with MHz order of natural linewidth. The only available transition for the ground-state Eu is the $a^8S_{7/2} - y^8P_{9/2}$, where the transition wavelength and the natural linewidth are 460 nm and 27 MHz, respectively. However, the Zeeman slowing of Eu is still challenging, since the values of the branching ratios from the excited state into metastable states are unknown. In this paper, we report measurement of the branching ratios from the excited state $y^8P_{9/2}$ to six metastable states through spectroscopy using an atomic beam. Based on the result, we discuss the possibility of the Zeeman slowing and magneto-optical trapping of Eu.

* Corresponding author.
E-mail address: kozuma@phys.titech.ac.jp (M. Kozuma).

http://dx.doi.org/10.1016/j.optcom.2017.01.059
Received 10 November 2016; Received in revised form 28 January 2017; Accepted 30 January 2017
Available online 04 February 2017

2. Optical leak problem

Europium has complex energy structure as well as Cr, Dy, and Er. Effective laser cooling of such atomic species is difficult because of the lack of closed optical transitions. When an atom is excited by absorption of a photon, in general, it has many decay channels to corresponding final (or metastable) states. For example, the $^7S_3-{}^7P_4$ transition is employed as a transition for the laser cooling of ^{52}Cr [26] and the excited state $^7P_4$ has two more relaxation pathways besides that to its ground state $^7S_3$. The probability of leakage out of the cooling transition limits the interaction-time or lifetime because the leakage transition turns off the cooling and trapping mechanism for the atom. Such a probability, which is usually referred to as an optical leak, is given by the sum of branching ratios to all final states except for one to the ground state. Here the branching ratio from the excited state to a particular final state labeled by i is defined as $\Gamma_i/\sum_{i'}\Gamma_{i'}$, where the Γ_i is the decay rate to the state i. The first MOT of ^{52}Cr is realized by repumping the leaked atoms back to the cooling transition [26], where the optical leak probability is 5×10^{-6} [27]. In the case of other dipolar atoms, ^{163}Dy and ^{168}Er also have the optical leak probabilities of 8×10^{-6} [28] and 7×10^{-6} [29], respectively. Despite such large optical leak probabilities, MOT of these atomic species is successfully demonstrated without any repumping beams. Since they have large magnetic dipole moments, atoms that decay to metastable states are trapped by quadrupole magnetic field used for the MOT and cascade back to their ground states in a few milliseconds [28,29].

In the case of Eu, the $a^8S_{7/2}-y^8P_{9/2}$ transition is the only feasible candidate to decelerate an atomic beam. Fig. 1 shows energy levels of Eu atoms up to 35000 cm^{-1} [30,31] with the $a^8S_{7/2}-y^8P_{9/2}$ transition. There are eleven electric-dipole transitions from the $y^8P_{9/2}$ excited state to metastable states. Among the eleven transitions, we measure branching ratios for three intercombination transitions ($y^8P_{9/2}-a^{10}D_{7/2,9/2,11/2}$, wavelength: 1148 ~ 1204 nm) and three allowed ones ($y^8P_{9/2}-a^8D_{7/2,9/2,11/2}$, wavelength: 1577 ~ 1760 nm). Note that the other five decays to the ignored states which have the longer transition wavelengths (4019 ~ 4880 nm) do not contribute to our estimation of the branching ratios as long as the decay rates to the ignored states are much smaller than that to the ground state. When we employ the $a^8S_{7/2}-y^8P_{9/2}$ as the cooling transition, the lower limit of the optical leak probability is given by the sum of the six branching ratios.

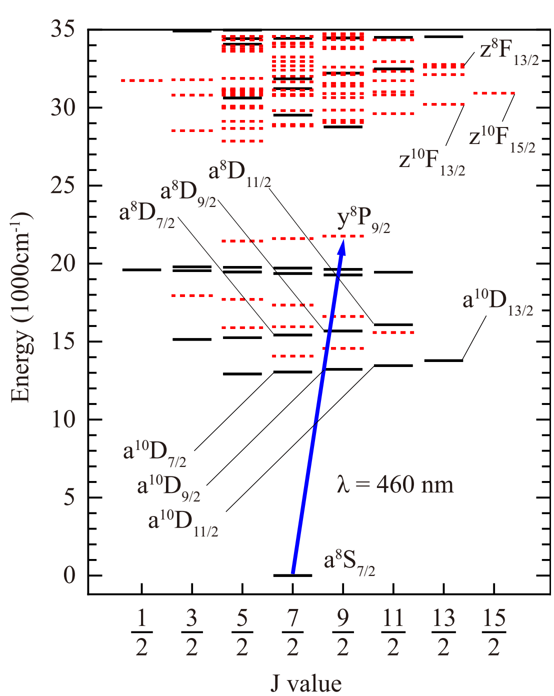

Fig. 1. Energy levels of europium, showing the $a^8S_{7/2}-y^8P_{9/2}$ transition. Solid (dotted) horizontal lines indicate odd (even) parity states. J is the total angular momentum.

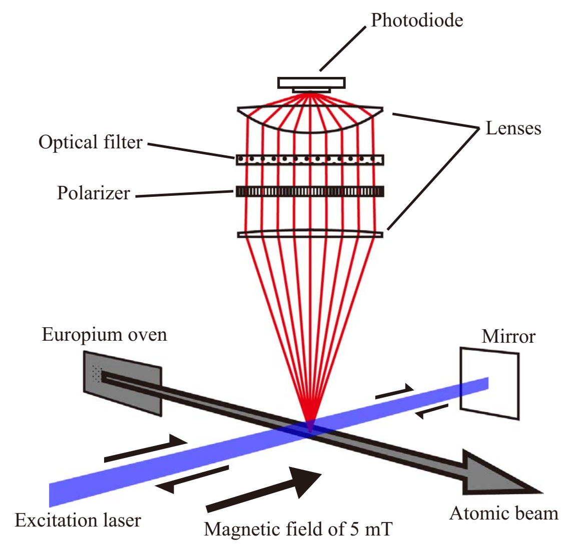

Fig. 2. Schematic of the experimental setup.

3. Experimental details

Fig. 2 shows the schematic of our experimental setup. The Eu atomic beam is produced by an effusive oven operating at 900 K. This temperature provides enough atomic density while keeping the background pressure of the chamber, where the laser and the atomic beam cross each other, is less than 1×10^{-4} Pa with the atomic beam running. The atoms have a mean longitudinal velocity of 360 m/s, and the transverse velocity profile was measured via fluorescence spectroscopy as Gaussian with a standard deviation of 4.4 m/s.

On-resonant light source for the $a^8S_{7/2}$ $(F=6)-y^8P_{9/2}$ $(F=7)$ transition at the wavelength of 460 nm is prepared by a frequency doubling with an external cavity laser diode at 919 nm. The circularly polarized laser beam crosses the atomic beam perpendicularly, where the Gaussian beam waist ($1/e^2$ intensity radius) and the peak intensity of the laser are 5 mm and 7 I_{sat}, respectively. Here, $I_{sat}=37$ mW/cm^2 denotes the saturation intensity for the transition. The excitation laser beam is counterpropagated in order to balance radiation pressure to the atomic beam. The fluorescence signal is obtained by sweeping the laser frequency across the resonance. The flux of the atoms in F=6 hyperfine manifold is 8.3×10^{11}/s, which is measured by absorption spectroscopy. The atoms are optically pumped to the m_F=6 magnetic sublevel at the upper stream of the atomic beam by circularly polarized light resonant to the $a^8S_{7/2}$ $(F=6)-y^8P_{9/2}$ $(F=7)$ transition with a parallel magnetic field of 0.5 mT.

Scattered photons at a wavelength of 460 nm are detected by a Si-PIN photodiode (Hamamatsu, S3399). The photons at infrared wavelengths, which correspond to relaxation channels into metastable states, are also detected by using InGaAs-PIN photodiodes (Hamamatsu, G12180-030A and G12181-230K, which have spectral response ranges of 900 – 1670 nm and 900 – 1850 nm, respectively). Fluorescence intensity is measured with each one of the following seven optical filters: four bandpass filters (center wavelengths are 1150 nm, 1200 nm, 1580 nm, 1650 nm, with the full width at half maximum of 10–12 nm), and three longpass filters (cut-on wavelengths are 750 nm, 1200 nm, 1400 nm), where the transmission spectrum of each filter is evaluated by Fourier transform infrared spectroscopy. Fig. 3 shows typical photocurrent signals at the wavelength of 460 nm (a) and at the infrared wavelength (b). Although some filters simultaneously pass the fluorescence corresponding to several decay channels, we can estimate the six branching ratios by using a maximum-likelihood

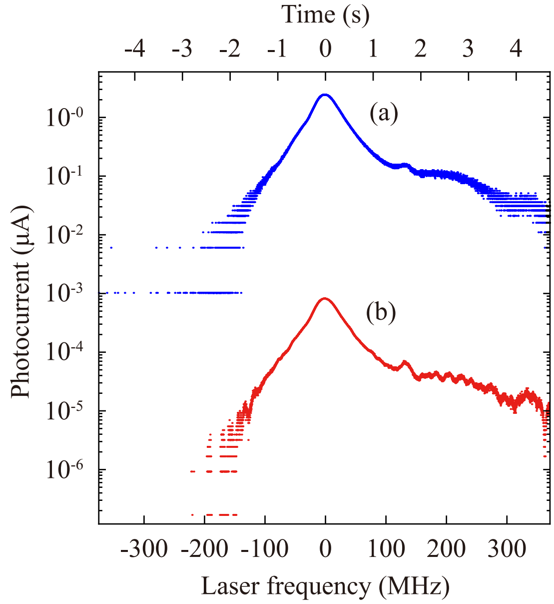

Fig. 3. Typical photocurrent signals corresponding to $\sigma_\pm$ polarized fluorescence at 460 nm (a) and at infrared wavelengths containing all the six transitions (b), plotted on a logarithmic scale.

method taking into account the wavelength dependence of the filters and the photodiodes. In the estimation, we ignore the other five decays whose wavelengths are longer than 4000 nm. The ignored fluorescence does not contribute to the measured photocurrent, since the quantum efficiency of the photodiodes is small enough at the wavelength range. Even if the ignored decay rates are comparable to the one to the six metastable states, the decay rates are still expected to be much smaller than one to the ground state. The systematic errors of the measured branching ratios caused by the ignorance are small enough as long as the branching ratios to the ignored decay channels are much smaller than unity.

Angular distributions of the fluorescence for individual optical transitions are generally anisotropic and different in each, whereas the signals only reflect a part of the fluorescence intensity due to a finite solid angle collection efficiency. In order to take into account this effects, we utilize the correspondence relation between the angular distribution and polarization of the fluorescence. The fluorescence intensities of two orthogonal polarization components are individually measured with rotating the linear polarizer shown in Fig. 2. Here we apply a magnetic field of 5 mT along the laser beam propagation direction, which we choose as the axis of quantization. The angular distributions of π and $\sigma_\pm$ polarization components are known to be proportional to $\sin^2\theta$ and $1+\cos^2\theta$, respectively, where θ is a polar angle with respect to the quantization axis. The polarization sensitive detection enables us to eliminate the polarization dependence in our estimation of the branching ratios. The branching ratios are also measured with linearly polarized excitation laser, and the results are consistent with the values with circularly-polarized excitation laser (listed in Table 1) within the experimental error; it confirms the validity of the scheme.

4. Results and discussion

The measured branching ratios from the $y^8\mathrm{P}_{9/2}$ excited state to the six metastable states are listed in Table 1. Here the number in the parentheses represents the uncertainty combining statistical and systematic errors. The primary sources of the errors are uncertainties of the optical filters' transmittances and those of quantum efficiencies for the photodiodes. The former comes from the dependence of the transmittance on the angle of the incident fluorescence light.

Table 1
Estimated branching ratios.

Transition ($y^8\mathrm{P}_{9/2}$ −)	Transition wavelength	Branching ratio
$a^{10}\mathrm{D}_{7/2}$	1148 nm	$0.32(6)\times10^{-4}$
$a^{10}\mathrm{D}_{9/2}$	1171 nm	$1.08(6)\times10^{-4}$
$a^{10}\mathrm{D}_{11/2}$	1204 nm	$1.78(6)\times10^{-4}$
$a^{8}\mathrm{D}_{7/2}$	1577 nm	$0.24(5)\times10^{-4}$
$a^{8}\mathrm{D}_{9/2}$	1644 nm	$1.33(6)\times10^{-4}$
$a^{8}\mathrm{D}_{11/2}$	1760 nm	$5.72(10)\times10^{-4}$
Total		$1.05(2)\times10^{-3}$

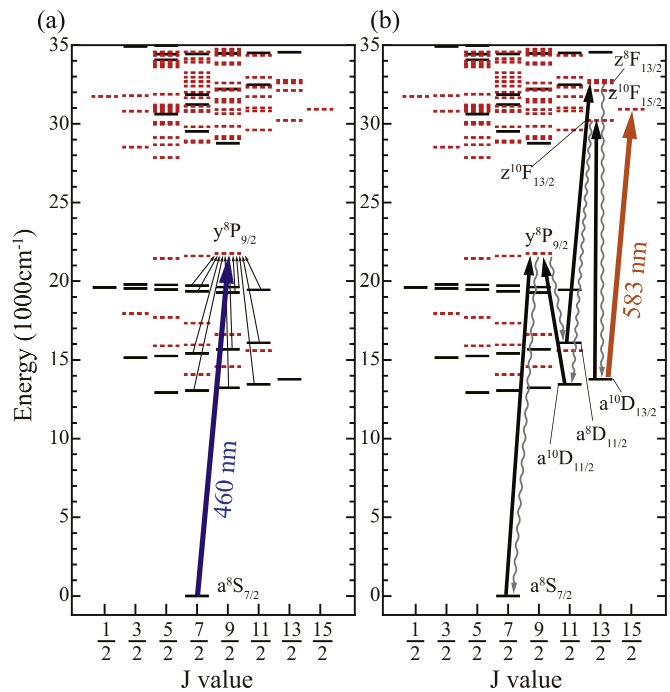

Fig. 4. The possible two schemes for laser cooling. (a) Laser cooling with repumping lights. (b) Laser cooling at metastable state with the optical pumping and pumping-back. Solid (dotted) horizontal lines indicate odd (even) parity states. The lasers needed for the scheme and resultant fluorescence are schematically shown by the bold and wave arrows, respectively.

The sum of the six branching ratios is $1.05(2)\times10^{-3}$, which is two orders of magnitude larger than the optical leak probabilities reported in the experiments using Cr [27], Dy [28], and Er [29]. As can be seen in Table 1, at least six repumping beams are required to reduce the optical leak probability to the same extent as the values for Cr, Dy and Er. Since there exist five more decay channels, eleven repumping lights are necessary to completely plug the all optical leaks. Fig. 4(a) shows the Eu energy level structure with the strongest laser cooling transition (460 nm) for magneto-optical trapping and Zeeman slowing, and with the required eleven repumping transitions.

Considering such large branching ratios, we here discuss the possibility to laser-cool Eu in the specific metastable state having a cyclic transition. Note that there are concerns about large two body losses for the ensemble of atoms in such a metastable state [32]. To perform the dipolar gas experiments with the condensate of Eu atoms, the atoms therefore should be pumped back to the ground state after the Zeeman slowing and MOT. The “pumping and pumping-back scheme” is schematically shown in Fig. 4(b), where all the associated lasers are depicted by the bold arrows. The transition $a^{10}\mathrm{D}_{13/2} - z^{10}\mathrm{F}_{15/2}$ is completely closed in electric-dipole approximation, where the wavelength and the natural linewidth are 583 nm and 8.3 MHz, respectively [31]. The cyclic transition with MHz order of natural linewidth can be applicable to conventional Zeeman slowing and MOT techniques. In order to prepare atoms in the $a^{10}D_{13/2}$ metastable state, we make use of the large branching ratios. One can start from pumping atoms in the ground state to the $a^8D_{11/2}$ metastable state by using the $a^8S_{7/2} - y^8P_{9/2}$ transition. On the basis of the branching ratios listed in Table 1, we estimate the best obtainable transfer efficiency to be 55%. Through successive optical pumping using the $a^8D_{11/2} - z^8F_{13/2}$ transition (wavelength: 599 nm), 92% of atoms in the $a^8D_{11/2}$ state can be pumped to the $a^{10}D_{13/2}$ state. Note that the optical pumping efficiency are calculated by using known decay rates [31], which are of the order of a few MHz. The total transfer efficiency from the ground state to the $a^{10}D_{13/2}$ metastable can thus be estimated to be 51%. In order to pump-back the laser-cooled atoms to its ground state, the $a^{10}D_{13/2} - z^{10}F_{13/2}$ transition (wavelength: 608 nm) and the $a^{10}D_{11/2} - y^8P_{9/2}$ transition (wavelength: 1204 nm) enables us to transfer the atoms with the efficiency of 95%. This scheme needs four additional light source (two for pumping, and the other two for pumping-back) except for the light source for the laser cooling transition.

5. Conclusion

We have spectroscopically measured the branching ratios from the $y^8P_{9/2}$ excited state to the six metastable states. The sum of the six branching ratios are estimated to be $1.05(2) \times 10^{-3}$, which indicates that laser-cooling of Eu atoms in the ground state requires at least six, maybe eleven repumping light sources. As a simpler alternative to preparing many repumping lights, we have also proposed the new scheme which utilizes the metastable state $a^{10}D_{13/2}$. The atoms can be efficiently pumped via all-optical way to the metastable state with the help of the large branching ratio. The $a^{10}D_{13/2} - z^{10}F_{15/2}$ transition enables us to operate the Zeeman slowing and MOT of the metastable Eu, and the laser-cooled atoms can also be pumped back to their ground state.

Acknowledgments

We sincerely thank B. P. Das for his valuable comments and many stimulating discussions. This work was supported by a Grant-in-Aid for Challenging Exploratory Research; the Murata Science Foundation, and the Research Foundation for Opto-Science and Technology.

References

[1] V.W. Scarola, S. Das Sarma, Quantum phases of the extended bose-hubbard hamiltonian: possibility of a supersolid state of cold atoms in optical lattices, Phys. Rev. Lett. 95 (2005) 033003. http://dx.doi.org/10.1103/PhysRevLett.95.033003.

[2] S. Yi, T. Li, C.P. Sun, Novel quantum phases of dipolar bose gases in optical lattices, Phys. Rev. Lett. 98 (2007) 260405. http://dx.doi.org/10.1103/PhysRevLett.98.260405.

[3] D. Peter, S. Müller, S. Wessel, H.P. Büchler, Anomalous behavior of spin systems with dipolar interactions, Phys. Rev. Lett. 109 (2012) 025303. http://dx.doi.org/10.1103/PhysRevLett.109.025303.

[4] A. de Paz, A. Sharma, A. Chotia, E. Maréchal, J.H. Huckans, P. Pedri, L. Santos, O. Gorceix, L. Vernac, B. Laburthe-Tolra, Nonequilibrium quantum magnetism in a dipolar lattice gas, Phys. Rev. Lett. 111 (2013) 185305. http://dx.doi.org/10.1103/PhysRevLett.111.185305.

[5] D.M. Stamper-Kurn, M. Ueda, Spinor bose gases: symmetries, magnetism, and quantum dynamics, Rev. Mod. Phys. 85 (2013) 1191–1244. http://dx.doi.org/10.1103/RevModPhys.85.1191.

[6] S. Yi, H. Pu, Spontaneous spin textures in dipolar spinor condensates, Phys. Rev. Lett. 97 (2006) 020401. http://dx.doi.org/10.1103/PhysRevLett.97.020401.

[7] Y. Kawaguchi, H. Saito, M. Ueda, Spontaneous circulation in ground-state spinor dipolar bose-einstein condensates, Phys. Rev. Lett. 97 (2006) 130404. http://dx.doi.org/10.1103/PhysRevLett.97.130404.

[8] M. Takahashi, S. Ghosh, T. Mizushima, K. Machida, Spinor dipolar bose-einstein condensates: classical spin approach, Phys. Rev. Lett. 98 (2007) 260403. http://dx.doi.org/10.1103/PhysRevLett.98.260403.

[9] A. Griesmaier, J. Werner, S. Hensler, J. Stuhler, T. Pfau, Bose-einstein condensation of chromium, Phys. Rev. Lett. 94 (2005) 160401. http://dx.doi.org/10.1103/PhysRevLett.94.160401.

[10] M. Lu, N.Q. Burdick, S.H. Youn, B.L. Lev, Strongly dipolar bose-einstein condensate of dysprosium, Phys. Rev. Lett. 107 (2011) 190401. http://dx.doi.org/10.1103/PhysRevLett.107.190401.

[11] K. Aikawa, A. Frisch, M. Mark, S. Baier, A. Rietzler, R. Grimm, F. Ferlaino, Bose-einstein condensation of erbium, Phys. Rev. Lett. 108 (2012) 210401. http://dx.doi.org/10.1103/PhysRevLett.108.210401.

[12] T. Lahaye, J. Metz, B. Fröhlich, T. Koch, M. Meister, A. Griesmaier, T. Pfau, H. Saito, Y. Kawaguchi, M. Ueda, d-Wave collapse and explosion of a dipolar bose-einstein condensate, Phys. Rev. Lett. 101 (2008) 080401. http://dx.doi.org/10.1103/PhysRevLett.101.080401.

[13] K. Aikawa, S. Baier, A. Frisch, M. Mark, C. Ravensbergen, F. Ferlaino, Observation of Fermi surface deformation in a dipolar quantum gas, Science 345 (6203) (2014) 1484–1487. http://dx.doi.org/10.1126/science.1255259.

[14] I. Ferrier-Barbut, H. Kadau, M. Schmitt, M. Wenzel, T. Pfau, Observation of quantum droplets in a strongly dipolar bose gas, Phys. Rev. Lett. 116 (2016) 215301. http://dx.doi.org/10.1103/PhysRevLett.116.215301.

[15] L. Chomaz, S. Baier, D. Petter, M.J. Mark, F. Wächtler, L. Santos, F. Ferlaino, Quantum-fluctuation-driven crossover from a dilute bose-einstein condensate to a macrodroplet in a dipolar quantum fluid, Phys. Rev. X 6 (2016) 041039. http://dx.doi.org/10.1103/PhysRevX.6.041039.

[16] H. Kadau, M. Schmitt, M. Wenzel, C. Wink, T. Maier, I. Ferrier-Barbut, T. Pfau, Observing the rosensweig instability of a quantum ferrofluid, Nature 530 (7589) (2016) 194–197. http://dx.doi.org/10.1038/nature16485.

[17] B. Laburthe-Tolra, Atomic physics: a strange kind of liquid, Nature 539 (7628) (2016) 176–177. http://dx.doi.org/10.1038/539176a.

[18] B. Pasquiou, E. Maréchal, G. Bismut, P. Pedri, L. Vernac, O. Gorceix, B. Laburthe-Tolra, Spontaneous demagnetization of a dipolar spinor bose gas in an ultralow magnetic field, Phys. Rev. Lett. 106 (2011) 255303. http://dx.doi.org/10.1103/PhysRevLett.106.255303.

[19] T. Maier, H. Kadau, M. Schmitt, M. Wenzel, I. Ferrier-Barbut, T. Pfau, A. Frisch, S. Baier, K. Aikawa, L. Chomaz, M.J. Mark, F. Ferlaino, C. Makrides, E. Tiesinga, A. Petrov, S. Kotochigova, Emergence of Chaotic Scattering in Ultracold Er and Dy, Phys. Rev. X 5 (2015) 041029. http://dx.doi.org/10.1103/PhysRevX.5.041029.

[20] S. Inouye, M.R. Andrews, J. Stenger, H.-J. Miesner, D.M. Stamper-Kurn, W. Ketterle, Observation of feshbach resonances in a bose-einstein condensate, Nature 392 (6672) (1998) 151–154. http://dx.doi.org/10.1038/32354.

[21] D.J. Papoular, G.V. Shlyapnikov, J. Dalibard, Microwave-induced fano-feshbach resonances, Phys. Rev. A 81 (2010) 041603. http://dx.doi.org/10.1103/PhysRevA.81.041603.

[22] T.M. Hanna, E. Tiesinga, P.S. Julienne, Creation and manipulation of Feshbach resonances with radiofrequency radiation, New J. Phys. 12 (8) (2010) 083031. http://dx.doi.org/10.1088/1367-2630/12/8/083031.

[23] J. Miao, J. Hostetter, G. Stratis, M. Saffman, Magneto-optical trapping of holmium atoms, Phys. Rev. A 89 (2014) 041401. http://dx.doi.org/10.1103/PhysRevA.89.041401.

[24] D. Sesko, T. Walker, C. Monroe, A. Gallagher, C. Wieman, Collisional losses from a light-force atom trap, Phys. Rev. Lett. 63 (1989) 961–964. http://dx.doi.org/10.1103/PhysRevLett.63.961.

[25] C.E. Habermann, Vapor Pressures of the Rare Earth Metals, (Ph.D. thesis), Iowa State University (1963).

[26] A.S. Bell, J. Stuhler, S. Locher, S. Hensler, J. Mlynek, T. Pfau, A magneto-optical trap for chromium with population repumping via intercombination lines, EPL (Europhys. Lett.) 45 (2) (1999) 156. http://dx.doi.org/10.1209/epl/i1999-00140-7.

[27] J. Stuhler, P.O. Schmidt, S. Hensler, J. Werner, J. Mlynek, T. Pfau, Continuous loading of a magnetic trap, Phys. Rev. A 64 (2001) 031405. http://dx.doi.org/10.1103/PhysRevA.64.031405.

[28] M. Lu, S.H. Youn, B.L. Lev, Trapping ultracold dysprosium: a highly magnetic gas for dipolar physics, Phys. Rev. Lett. 104 (2010) 063001. http://dx.doi.org/10.1103/PhysRevLett.104.063001.

[29] J.J. McClelland, J.L. Hanssen, Laser cooling without repumping: a magneto-optical trap for erbium atoms, Phys. Rev. Lett. 96 (2006) 143005. http://dx.doi.org/10.1103/PhysRevLett.96.143005.

[30] W.C. Martin, R. Zalubas, L. Hagan, Atomic energy levels – the rare-earth elements, National Standard Reference Data Series Vol. 60 (NBS, Washington, D.C., 1978).

[31] E.A.D. Hartog, M.E. Wickliffe, J.E. Lawler, Radiative lifetimes of Eu I, II, and III and transition probabilities of Eu I, Astrophys. J. Suppl. Ser. 141 (1) (2002) 255. http://dx.doi.org/10.1086/340039.

[32] W. Vassen, C. Cohen-Tannoudji, M. Leduc, D. Boiron, C.I. Westbrook, A. Truscott, K. Baldwin, G. Birkl, P. Cancio, M. Trippenbach, Cold and trapped metastable noble gases, Rev. Mod. Phys. 84 (2012) 175–210. http://dx.doi.org/10.1103/RevModPhys.84.175.